Applied Physics Letters

Hybrid states of a cavity-photon–vortex coupled system in a superconductive cavity

Cite as: Appl. Phys. Lett. **121**, 194002 (2022); https://doi.org/10.1063/5.0123823
Submitted: 01 September 2022 • Accepted: 27 October 2022 • Published Online: 10 November 2022

Lei Wang, Xin Shang, Haiwen Liu, et al.

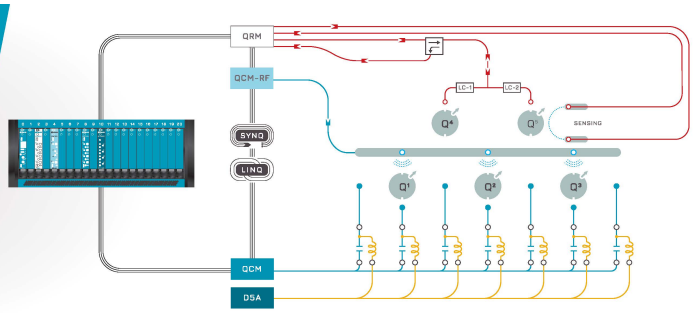

AIP Publishing

Applied Physics Letters ARTICLE scitation.org/journal/apl

Hybrid states of a cavity-photon–vortex coupled system in a superconductive cavity

Cite as: Appl. Phys. Lett. **121**, 194002 (2022); doi: 10.1063/5.0123823
Submitted: 1 September 2022 · Accepted: 27 October 2022 ·
Published Online: 10 November 2022

Lei Wang,[1,a)] Xin Shang,[2] Haiwen Liu,[3] Tai Min,[1] and Ke Xia[4,a)]

AFFILIATIONS

[1]Center for Spintronics and Quantum Systems, State Key Laboratory for Mechanical Behavior of Materials, Xi'an Jiaotong University, 28 Xianning West Road Xi'an, Shaanxi 710049, China
[2]Beijing Computational Science Research Center, Beijing 100193, China
[3]The Center for Advanced Quantum Studies and Department of Physics, Beijing Normal University, Beijing 100875, China
[4]School of Physics, Southeast University, Nanjing 211189, China

[a)]**Authors to whom correspondence should be addressed:** wanglei.icer@xjtu.edu.cn and kexia@csrc.ac.cn

ABSTRACT

As the Abrikosov vortex lattice has recently been found in van der Waals heterostructures constructed by a two-dimensional (2D) ferromagnet and a superconductor, we propose the realization of cavity-photon–vortex coupling in a superconductive cavity to construct a new hybrid quantum system in this paper. We study the corresponding hybrid states therein, including the exceptional lines (ELs) in the parameter space. Considering that the parameters of our system are adjustable by external magnetic field and temperature, our system and the ELs are much easier to be realized in experiments. Furthermore, the numerical results show that the corresponding hybrid states can be switched by tuning the source of AC, which makes this hybrid system more advantageous to realize hybrid quantum computing in the future. Moreover, for practical use in detecting hybrid states and the vortex dynamics, the transmission amplitude of an external transverse electric wave through the cavity is also studied.

Hybrid quantum systems have attracted increasing attention in quantum technologies because the combination of two or more physical systems can merge the advantages of different components for better performance.[1] The key to such systems is mainly sorted into two aspects: one is the strong coupling strength for fast and effective operation and the other is the high quality factor for low energy dissipation and long lifetime.

A cavity is an efficient object to realize hybrid quantum systems between cavity-photon and other physical systems, such as magnons and superconducting qubits.[2–4] Moreover, as magnons can be directly coupled with the cavity-photon in a cavity, cavity-photon–magnon systems have become a promising platform for quantum technologies, as demonstrated by both experimental[5–13] and theoretical[14–18] works. However, the corresponding coupling strength in the traditional cavity is essentially small because the coupling scales with the square root of the number of spins in the system per volume of the microwave cavity.[7,19] To amplify the coupling strength, a superconductive cavity was proposed,[20,21] in which a several orders of magnitude enhancement was achieved.[21] In this sense, the superconductive cavity could be a better candidate for a strongly coupled hybrid quantum system.

Recently, two-dimensional (2D) topological superconductivity was proposed in van der Waals heterostructures constructed by a 2D ferromagnet and a superconductor,[22] and the vortex lattice, therein, was accordingly observed.[23] As the 2D van der Waals heterostructure provides a high-quality interface and an easily regulated nature through multiple external methods,[24–28] such a system combined with a cavity can potentially be integrated into devices and chips for hybrid quantum computing in the future.[3]

Moreover, the quality factor of the vortex oscillation is dependent on the viscosity coefficient η, the restoring force constant κ, and the working frequency (ω),[29] which represents the operating frequency of the device and is determined by the AC, as shown in Fig. 1. For a typical superconductor $YBa_2Cu_3O_7$, η is on the order of $10^{-6}\,\mathrm{N\,s\,m^{-2}}$, and κ is on the order of $10^5\,\mathrm{N\,m^{-2}}$;[30] thus, the corresponding quality factor at $\omega = 1\,\mathrm{MHz}$ could be as large as $Q_v = 10^{10}$, which is much larger than that of the cavity optomechanic[2,31] and the optomagnonic[8,32] systems. In addition, we can define the maximum working frequency of the vortex oscillation by the point of half power absorption of supercurrents relative to a DC, reading $\omega_{vt} = \kappa/\eta$. In this sense, the corresponding ω_{vt} can be up to 100 GHz. Considering that

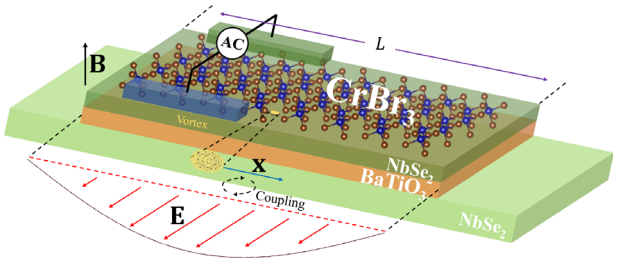

FIG. 1. Model of the coupling between the transverse electric (TE) wave and the vortex in the top type-II superconductor. Here, "AC" indicates that a driving force is applied via an alternating current (AC) with frequency ω_{AC}, L is the length of the cavity constructed by $NbSe_2/BaTiO_3/NbSe_2$, $\mathbf{x}$ denotes the location of the vortex driven by the Lorentz force, $\mathbf{E}$ is the electric field component of the TE wave with wavelength $\lambda = 2L$, representing a $\lambda/2$ resonator, and $\mathbf{B}$ is the external magnetic field to introduce the flux quanta in $NbSe_2$.

the quantum ground state cooling temperature limit is generally defined as $T \ll \hbar\omega_{vt}/k_B$, the ultra-high frequency of the vortex oscillation leads to the higher quantum ground state cooling temperature compared to that of the optomagnonic and optomechanics systems.[33,34] One may also note that κ is related to the external magnetic field[35] and temperature,[35,36] η also depends on the temperature,[37–39] and the working frequency of vortex oscillation can be tuned in the range of $0 \sim \omega_{vt}$; therefore, the frequency matching between the vortex oscillation and the cavity-photon should be convenient. The above-mentioned large Q_v and broad working frequency window make the vortex an efficient candidate in hybrid quantum systems.

These experimental results inspire us to propose a cavity-photon–vortex hybrid quantum system in a superconductive cavity. As the vortex is driven by the Lorentz force arising from the supercurrent in superconductors, it can be directly coupled to the electric field component of the cavity-photon. Thus, the coupling strength should be stronger, and the experimental realization should be easier. In this sense, the study of the cavity-photon–vortex coupling in a superconductive cavity should be of great importance.

To study the coupling between the cavity-photon and the vortex, a brief model is setup, as shown in Fig. 1. Technically, one may construct the cavity by fabricating a dielectric layer (e.g., $BaTiO_3$) sandwiched by two superconductor layers (e.g., $NbSe_2$) with a finite length of L. Under this condition, the intrinsic frequency of the cavity can be obtained by $\omega_{cav} = 2\pi f = \pi\bar{c}/L$ for a half-wavelength resonator ($\lambda = 2L$), where $\bar{c}$ is the Swihart velocity, which reads[21,40]

$$\bar{c} = c_0\sqrt{d_I/\varepsilon_I(2\lambda_L + d_I)}, \tag{1}$$

where c_0 is the velocity of light in vacuum; d_I and ε_I are the thickness and dielectric constant of the dielectric layer, respectively; and λ_L is the London penetration depth of the superconductor layer. For a certain cavity of $NbSe_2/BaTiO_3/NbSe_2$, the above-mentioned parameters can be accordingly set as $d_I = 3$ nm, $\varepsilon_I = 7000$,[41] and $\lambda_L \simeq 0.5$ μm.[42,43] Thus, $\bar{c} \simeq 6.5 \times 10^{-4}c_0$, and when $L \simeq 6$ mm, the intrinsic frequency of the cavity ω_{cav} is on the order of 100 MHz.

For the generation of the vortex,[22,23] we chose the $CrBr_3/NbSe_2$ heterostructure as an example, as shown in Fig. 1. Considering that the vortex lattice is a result of the mixed state in the type-II superconductors, which is a regular lattice of magnetic flux quanta, an external magnetic field $\mathbf{B}$ is also needed. Meanwhile, the vortex can be driven by an external alternating current (AC) source with a finite frequency ω_{AC} and then couple with the electric field component ($\mathbf{E}$) of the cavity-photon, which is the $\lambda/2$ resonator of a transverse electric (TE) wave, as shown in Fig. 1. As the wavelength of the TE wave is much larger than the amplitude of the vortex dynamics, the electric field around the vortex is treated homogeneously with a constant frequency ω_{cav} determined by the cavity.

In general, the vortex can be treated as a quasiparticle and as the displacements of the vortices driven by the supercurrent are approximately the same, the corresponding forces between vortices will be negligible.[44] Therefore, the vortex dynamics can be governed by a phenomenological equation for a single vortex, which reads[44,45]

$$\eta\dot{\mathbf{x}} + \kappa\mathbf{x} = \mathbf{J}_s\frac{\psi_0}{c}, \tag{2}$$

where $\mathbf{x} = x_0e^{-i\omega t}$ is the location of the vortex, $\mathbf{J}_s$ is the supercurrent to drive the vortex by the Lorentz force, and $\psi_0 = hc/2e$ is the flux quantum.

The supercurrent can be separated into two independent parts: one part is the external AC, as shown in Fig. 1, $\mathbf{J}_d = J_0e^{-i\omega_{AC}t}$, which is used to drive the vortex, and the other part is from the electric field component of the cavity-photon, which can be written as an electric field response. Using the first London equation, it reads

$$\mathbf{J}_L = \frac{1}{-i\omega\Lambda}\mathbf{E}, \tag{3}$$

where $\mathbf{E} = E_0e^{-i\omega t}$ and $\Lambda = m^*/n^*q^*q^*$ with effective mass $m^* = 2m_e$, effective charge $q^* = 2q_e$, and effective density $n^* = n/2$ of the Cooper pair in the superconductors. The driving force from $\mathbf{J}_d$ can be treated independently as a control of the vortex oscillation frequency. Thus, we have

$$(-i\omega_{AC}\eta + \omega_{vt}\eta)\mathbf{x} = \mathbf{J}_d\frac{\psi_0}{c}. \tag{4}$$

Moreover, there could be a ratio C_r between the amplitudes of $\mathbf{J}_L$ and $\mathbf{J}_d$ and accordingly a phase difference ϕ. The phase difference ϕ can be controlled by adding an extra phase shift voltage regulation circuit into the system. Then, the vortex dynamics are given by

$$\eta(\omega^2 - \omega_{AC}\omega)\mathbf{x} + \mathcal{C}e^{-i\phi}\mathbf{E} = 0, \tag{5}$$

where $\mathcal{C} = \frac{C_r}{\Lambda}\frac{h}{2e}$. If there is no cavity ($\mathbf{E} = 0$), then the frequency of the vortex oscillation will be exactly the frequency (ω_{AC}) of the driving force from $\mathbf{J}_d$, which obeys the rule of forced vibration.

The cavity-photon can be described by a general LCR equation,[8,16,18,32,47] which reads

$$\mathscr{L}\dot{\mathbf{J}}_n + \mathscr{R}\mathbf{J}_n + \frac{1}{\mathscr{C}}\int\mathbf{J}_n dt = \mathbf{V}^F, \tag{6}$$

where $\mathbf{J}_n$ is the current and $\mathbf{V}^F$ is the driving force from the feedback of the vortex dynamics. In an LCR circuit, we have $\mathbf{J}_n = \mathbf{V}_c/X_c$, where $\mathbf{V}_c = \mathbf{E}d_c$ is the voltage on the capacitor, with d_c being the corresponding distance and $X_c = 1/\omega\mathscr{C}$ being the corresponding impedance. Therefore, $\mathbf{J}_n = \omega\mathscr{C}d_c\mathbf{E}$. Moreover, the driving force comes from the voltage drop induced by the motion of the magnetic flux quanta, which can be simply written as[48]

$$\mathbf{V}^F = -K\dot{\mathbf{x}} = iK\omega\mathbf{x}, \tag{7}$$

where $K = (h/2e)^2 L n_f |\mathbf{J}_d|$ with n_f being the density of the free vortex. Define the intrinsic frequency of the LCR circuit as $\omega_{cav} = \frac{1}{\sqrt{\mathscr{L}\mathscr{C}}}$, the corresponding damping as $\beta = \frac{\mathscr{R}}{2\mathscr{L}\omega_{cav}}$, and the normalized coupling strength as $\mathcal{K} = K/d_c$; Eq. (6) becomes

$$\mathcal{K}\omega_{cav}^2\omega\mathbf{x} + (\omega^2 + 2i\beta\omega_{cav}\omega - \omega_{cav}^2)\mathbf{E} = 0. \tag{8}$$

Combining Eqs. (5) and (8) and considering $\omega > 0$ for physical results, we have the following linear equations:

$$\Omega \times \begin{pmatrix} \mathbf{x} \\ \mathbf{E} \end{pmatrix} = 0, \tag{9}$$

where

$$\Omega = \begin{pmatrix} \omega - \omega_{AC} & \mathcal{P}e^{-i\phi} \\ \dfrac{\omega_{cav}^2}{\omega + \sqrt{1-\beta^2}\omega_{cav} + \beta\omega_{cav}i} & \omega - \sqrt{1-\beta^2}\omega_{cav} + \beta\omega_{cav}i \end{pmatrix}, \tag{10}$$

with $\mathcal{P} = \frac{\mathcal{K}\mathcal{C}}{\eta}$ being the coupling constant. By diagonalizing the matrix Ω, we obtain the frequency spectrum.

Here, one should notice that the coupling constant $\mathcal{P}$ mainly comes from two parts: one is the response between the supercurrent and the electric field component of the TE wave in the cavity ($\mathcal{C}/\eta$), and the other is the voltage drop induced by the motion of the vortex ($\mathcal{K}$). By submitting all parameters, we have

$$\mathcal{P} = \frac{h^3 L n_f |\mathbf{J}_d| C_r}{8e^3 d_c \eta \Lambda}. \tag{11}$$

For a $NbSe_2$ thin film, the parameters can be obtained as follows: an experimental observed $n_f \simeq 400/\mu m^2$;[49] an estimated $\Lambda \simeq 2.8 \times 10^{-9}$ kg $\mathscr{C}^{-2}$ cm^2 with the carrier density $n = 1.25 \times 10^{16}$ cm^{-2};[50] and as the critical current in $NbSe_2$ is reported to be on the order of mA on a sample with a 0.0018×0.4 mm^2 lateral area,[51] we set $\mathbf{J}_d = 10^6$ A·m^{-2} typically. Moreover, as described previously, $L = 6$ mm and η is on the order of 10^{-6} N·s·m^{-2}.[30] Thus, if we choose $C_r = 1$ for a general device without tuning the amplitude of the supercurrents and $d_c \simeq 100\ \mu$m for a typical width of the device, the initialized coupling parameter will be $\mathcal{P}_0 \simeq 7.6 \times 10^{-4}$ N/s. We also notice that $\mathcal{P}$ can be tuned in multiple ways, especially the source of the AC ($|\mathbf{J}_d|$ and C_r) and the temperature related viscosity coefficient η,[37–39] which make $\mathcal{P}$ vary in orders of magnitude.

In addition, we set the general damping of the cavity $\beta = 0.002$;[8,16,46] then, the spectrum can be obtained as shown in the upper panel of Fig. 2. Here, we should notice that as the frequency of the AC (ω_{AC}) is much easier to control in experiments, we mainly vary the ω_{AC} with fixing the intrinsic frequencies of the cavity (ω_{cav}) to solve the eigenvalues (ω) of the hybrid quantum system. When $\mathcal{P} = 0$ for the decoupled condition, a constant eigenvalue [$Re(\omega) = \omega_{cav}\sqrt{1-\beta^2} \simeq \omega_{cav}$] of the cavity and a linearized eigenvalue ($\omega = \omega_{AC}$) of the vortex dynamics clearly appear. Moreover, when $\mathcal{P} \neq 0$, the coupled anticrossing mode appears, and the phase difference ϕ can accordingly change the shape of the curves. Specifically, when $\mathcal{P} = \mathcal{P}_0$ and $\phi = \pi$, a crossing point appears at $\omega_{AC} = \omega_{cav}$. To further understand the influence of the parameters,

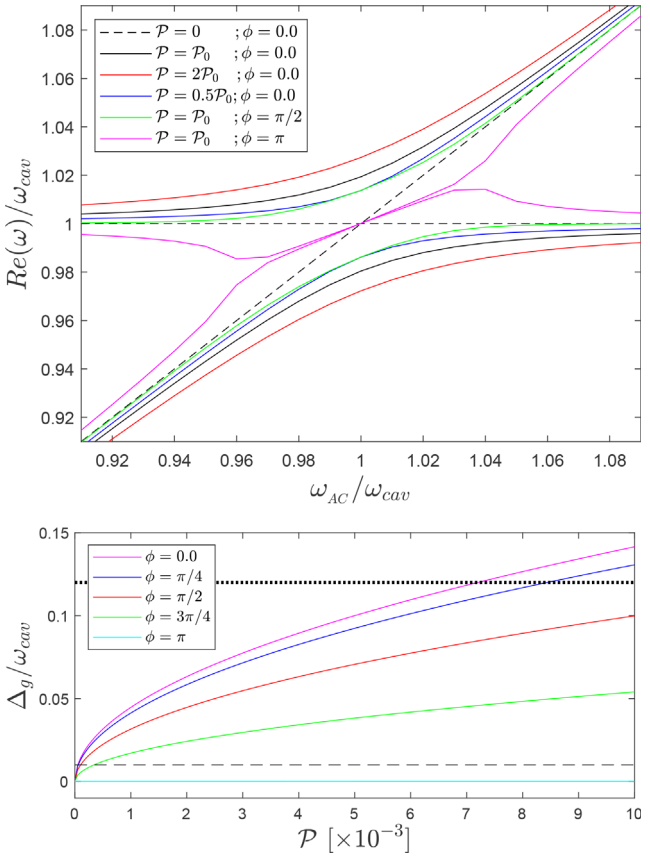

FIG. 2. Upper panel: spectrum obtained by diagonalizing the matrix Ω with various parameters. Lower panel: bandgaps (Δ_g) as a function of the coupling parameter $\mathcal{P}$ for various phase differences ϕ, when the frequency of the AC equals to the intrinsic frequency of the cavity ($\omega_{AC} = \omega_{cav}$). Here, the dashed and dotted lines represent the Δ_g of the conventional[46] and superconductive[21] cavity-photon–magnon systems, respectively.

we also calculate the band gaps (Δ_g) with various parameters when $\omega_{AC} = \omega_{cav}$, as shown in the lower panel of Fig. 2. With these results, we can conclude that Δ_g is proportional to $\mathcal{P}$ but suppressed by the phase difference ϕ.

Another important issue for the hybrid states of non-Hermitian systems are the ELs in parameter space, which are constructed by consecutive exceptional points (EPs). For the hybrid states at the EPs, there are multiple intriguing phenomena to be observed, e.g., unidirectional invisibility,[52–55] unidirectional energy transfer,[56] single-mode lasing,[57] loss-induced lasing,[58] and ultrahigh sensitivity.[59] However, in experiments, it is hard to realize the EPs due to the precisely controlled parameters. For example, (1) in the optomagnonic systems, it is needed to move the location of the YIG sphere inside the open cavity to adjust the coupling strengths to achieve the "nonreciprocity and unidirectional invisibility" at EPs[54] and (2) the working frequency is fixed for a given device to obtain ultra-high sensitivity for magnetometers.[59]

In general, the ELs can be captured by simply analyzing whether the imaginary part of the eigenvalues of the hybrid states equal zero. Thus, we show the eigenvalues of the hybrid states within a ϕ-ω_{AC}

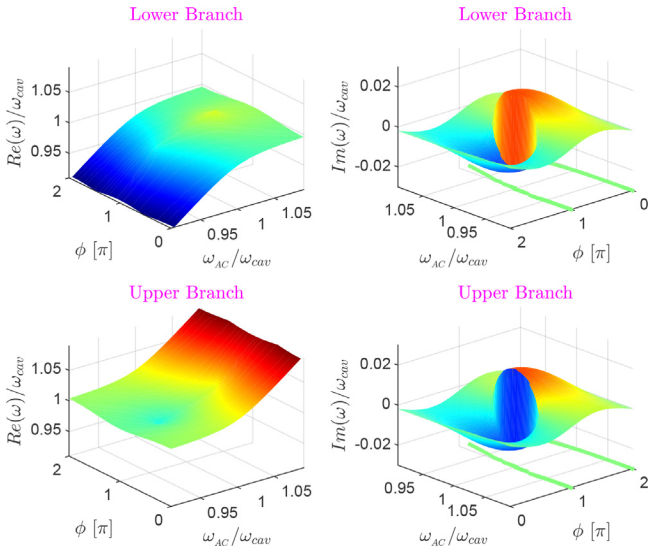

FIG. 3. The eigenvalues of Ω with $\mathcal{P} = \mathcal{P}_0$ and $\beta = 0.002$ for various ϕ and ω_{AC}, where the upper and lower branches represent the corresponding bands when $\omega > \omega_{cav}$ and $\omega < \omega_{cav}$, respectively. The green lines at the bottom of the subfigures are the corresponding projected contours with $Im(\omega)/\omega_{cav} = 0$, representing the exceptional lines (ELs), accordingly.

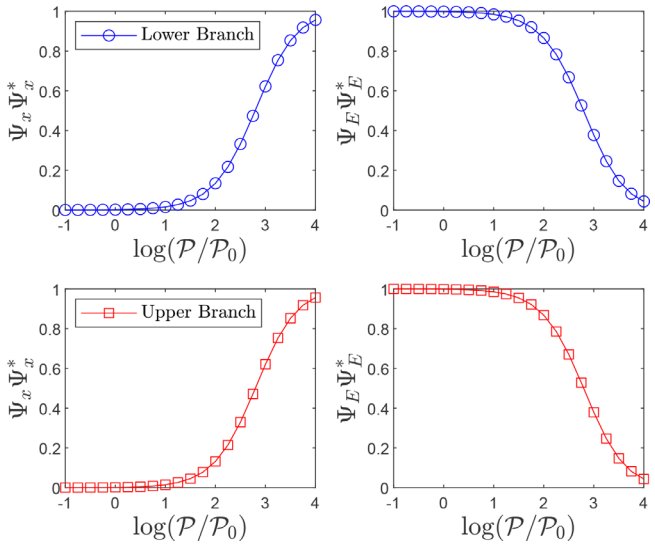

FIG. 4. The components of the hybrid states vs $\mathcal{P}$ with $\omega_{AC} = \omega_{cav}$ and $\phi = \pi$ for the two anticrossing branches, as shown in Fig. 2. Here, Ψ_x and Ψ_E represent the eigenvectors of the vortex oscillation and TE wave in the cavity, respectively.

space in Fig. 3, together with contours (green lines at the bottom) to show the location of the corresponding ELs, where the ELs are mainly located around $\phi = 0, \pi, 2\pi$ with a slightly distortion. Considering that the related parameters in our system ($\mathcal{P}$, κ, η, ω_{AC}, and ϕ) could be changed by tuning the external magnetic field, temperature, or the AC outside the cavity, it should be much easier to find the EPs in our system. Due to the existence of the ELs in ϕ-ω_{AC} space, one may feel free to control the working frequencies.

Furthermore, considering that the control of the hybrid states is the key to technically realizing the "computing" in the future,[3,60] e.g., a NOT gate, the switching of the hybrid states should be of great importance. Here, we notice that the effective coupling parameter $\mathcal{P}$ can be tuned in multiple ways as described previously, such as the AC related $|\mathbf{J}_d|$, C_r, and the temperature related viscosity coefficient η.[37–39] Considering that the AC can be easily tuned by the source, the AC control of the hybrid states could be much easier to be realized in applications. In this sense, we calculate the $\mathcal{P}$-dependent components of the corresponding hybrid states, as shown in Fig. 4, where Ψ_x and Ψ_E stand for the eigenvectors of the vortex oscillation and TE wave in the cavity, respectively. It can be seen that, when increasing $\mathcal{P}$, the component of vertex oscillation increases while the component of the TE wave decreases, indicating a hybrid state switching.

For experimental observation of these coupled states, the transmission amplitude of an external microwave is needed.[8,16,18,32] Thus, we should obtain the corresponding formula. Technically, if we inject an external TE wave through the whole device, then there will be another driving force on the LCR circuit, which can be qualitatively written as

$$\mathbf{V}^{TE} \equiv d_c \mathbf{E}_0. \tag{12}$$

Substituting this into Eq. (6), we have the following revised equation:

$$\mathcal{K}\omega_{cav}^2\omega\mathbf{x} + (\omega^2 + 2i\beta\omega_{cav}\omega - \omega_{cav}^2)\mathbf{E} = i\omega_{cav}^2\mathbf{E}_0, \tag{13}$$

and the corresponding Eq. (9) becomes

$$\Omega\begin{pmatrix}\mathbf{x}\\ \mathbf{E}\end{pmatrix} = \begin{pmatrix} 0 \\ \dfrac{i\omega_{cav}^2}{\omega + \sqrt{1-\beta^2}\omega_{cav} + \beta\omega_{cav}i}\mathbf{E}_0 \end{pmatrix}. \tag{14}$$

In this case, the transmission amplitude will be

$$S_{21} = \Gamma\frac{\mathbf{E}}{\mathbf{E}_0} = \frac{i\omega_{cav}^2\Gamma}{\omega + \sqrt{1-\beta^2}\omega_{cav} + \beta\omega_{cav}i}\frac{\omega - \omega_{AC}}{det\Omega}, \tag{15}$$

with $\Gamma = 2\beta$ characterizing the cavity/cable impedance mismatch.

Using the above-mentioned formulas, the transmission amplitude $|S_{21}|^2$ with various parameters can be obtained, as shown by the color area in Fig. 5, together with the corresponding spectrum of the coupled system plotted by the red dashed lines. When $\phi = 0$, the usual anticrossing features are observed. Distinctly, when $\phi = \pi$, the patterns become different and form abnormal anticrossing features, with the gap proportional to $\mathcal{P}$. This abnormal feature can be captured as follows: S_{21} always reaches a maximum value around the eigenvalues (red dashed lines) due to the resonance between the cavity-photon–vortex hybrid states and the input TE wave; however, according to Eq. (15), when $\omega = \omega_{AC}$, $S_{21} = 0$ in any case. Therefore, the transmission amplitude will be zero around the line of $\omega = \omega_{AC}$, which opens the gap and leads to abnormal anticrossing patterns, as shown in Fig. 5. Moreover, when $\beta = 0.0001$, the eigenvalues inside the gap will become degenerate. However, this state is too sensitive to the phase difference ϕ, as observed in Fig. 5; if $\phi = 5\pi/6$, then eigenvalues are generated inside the gap, forming parallel bands, as shown by the corresponding red dashed lines, and the pattern of $|S_{21}|^2$ accordingly changes.

In summary, we propose a two-oscillator model to describe the coupling between the cavity-photon and the vortex oscillation in a

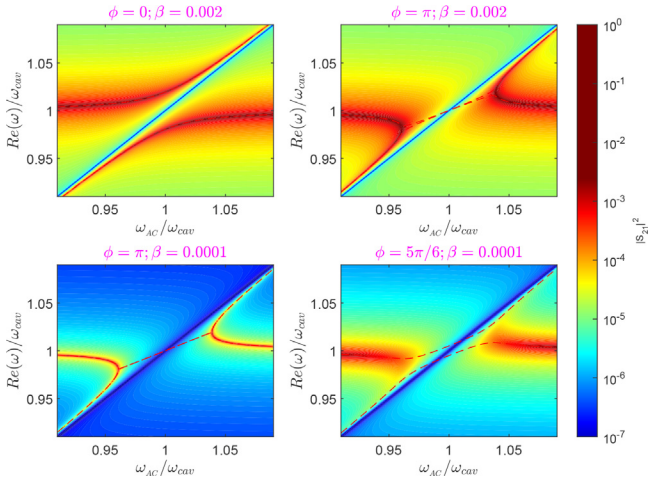

FIG. 5. The color area represents the transmission amplitude $|S_{21}|^2$ for various ϕ and β with $\mathcal{P} = \mathcal{P}_0$. The red dashed lines are the corresponding spectrum of the coupled system obtained by diagonalizing the matrix Ω.

superconductive cavity and study the hybrid states therein, including the corresponding ELs. Considering that our parameter space is adjustable by external magnetic field and temperature, our system should be much easier to be realized in experiments. Moreover, we observe a usual anticrossing mode when there is no phase difference ($\phi = 0$) between the external driving current and the electric field component of the cavity-photon. When $\phi = \pi$, a different coupling mode appears with an abnormal anticrossing feature. In particular, the corresponding hybrid states can be switched by controlling the source of AC, which is much easier to be realized in the future. For detection of the hybrid states and the vortex dynamics, we investigate the transmission amplitude through the cavity for different coupling modes by injecting an external TE wave.

This work was financially supported by the National Key R&D Program of China (Grant No. 2021YFA1202200) and the China Postdoctoral Science Foundation (Grant No. 2021T140549). K.X. was supported by the National Natural Science Foundation of China (Grant No. 11734004).

AUTHOR DECLARATIONS

Conflict of Interest

The authors have no conflicts to disclose.

Author Contributions

Lei Wang: Data curation (lead); Formal analysis (equal); Funding acquisition (equal); Investigation (lead); Methodology (lead); Project administration (equal); Supervision (equal); Visualization (lead); Writing – original draft (lead); Writing – review & editing (equal). **Xin Shang:** Formal analysis (equal); Investigation (equal); Methodology (equal). **Haiwen Liu:** Formal analysis (equal); Investigation (equal); Methodology (equal); Supervision (supporting); Writing – review & editing (supporting). **Tai Min:** Formal analysis (supporting); Supervision (equal). **Ke Xia:** Conceptualization (lead); Formal analysis (equal); Investigation (equal); Methodology (equal); Supervision (lead); Writing – review & editing (equal).

DATA AVAILABILITY

The data that support the findings of this study are available from the corresponding authors upon reasonable request.

REFERENCES

[1]Z.-L. Xiang, S. Ashhab, J. Q. You, and F. Nori, Rev. Mod. Phys. **85**, 623 (2013).
[2]M. Aspelmeyer, T. J. Kippenberg, and F. Marquardt, Rev. Mod. Phys. **86**, 1391 (2014).
[3]D. Lachance-Quirion, Y. Tabuchi, A. Gloppe, K. Usami, and Y. Nakamura, Appl. Phys. Express **12**, 070101 (2019).
[4]H. Y. Yuan, Y. Cao, A. Kamra, R. A. Duine, and P. Yan, "Quantum magnonics: When magnon spintronics meets quantum information science," arXiv:2111.14241 [quant-ph] (2021).
[5]H. Huebl, C. W. Zollitsch, J. Lotze, F. Hocke, M. Greifenstein, A. Marx, R. Gross, and S. T. B. Goennenwein, Phys. Rev. Lett. **111**, 127003 (2013).
[6]X. Zhang, C.-L. Zou, L. Jiang, and H. X. Tang, Phys. Rev. Lett. **113**, 156401 (2014).
[7]Y. Tabuchi, S. Ishino, T. Ishikawa, R. Yamazaki, K. Usami, and Y. Nakamura, Phys. Rev. Lett. **113**, 083603 (2014).
[8]L. Bai, M. Harder, Y. P. Chen, X. Fan, J. Q. Xiao, and C.-M. Hu, Phys. Rev. Lett. **114**, 227201 (2015).
[9]R. Hisatomi, A. Osada, Y. Tabuchi, T. Ishikawa, A. Noguchi, R. Yamazaki, K. Usami, and Y. Nakamura, Phys. Rev. B **93**, 174427 (2016).
[10]N. Kostylev, M. Goryachev, and M. E. Tobar, Appl. Phys. Lett. **108**, 062402 (2016).
[11]Y.-P. Wang, G.-Q. Zhang, D. Zhang, X.-Q. Luo, W. Xiong, S.-P. Wang, T.-F. Li, C.-M. Hu, and J. Q. You, Phys. Rev. B **94**, 224410 (2016).
[12]Y.-P. Wang, G.-Q. Zhang, D. Zhang, T.-F. Li, C.-M. Hu, and J. Q. You, Phys. Rev. Lett. **120**, 057202 (2018).
[13]J. Zhao, L. Wu, T. Li, Y.-X. Liu, F. Nori, Y. Liu, and J. Du, Phys. Rev. Appl. **15**, 024056 (2021).
[14]O. O. Soykal and M. E. Flatté, Phys. Rev. Lett. **104**, 077202 (2010).
[15]Y. Cao, P. Yan, H. Huebl, S. T. B. Goennenwein, and G. E. W. Bauer, Phys. Rev. B **91**, 094423 (2015).
[16]V. L. Grigoryan, K. Shen, and K. Xia, Phys. Rev. B **98**, 024406 (2018).
[17]W. Yu, T. Yu, and G. E. W. Bauer, Phys. Rev. B **102**, 064416 (2020).
[18]V. L. Grigoryan and K. Xia, Phys. Rev. B **102**, 064426 (2020).
[19]G. S. Agarwal, Phys. Rev. Lett. **53**, 1732 (1984).
[20]I. Golovchanskiy, N. Abramov, V. Stolyarov, V. Chichkov, M. Silaev, I. Shchetinin, A. Golubov, V. Ryazanov, A. Ustinov, and M. Kupriyanov, Phys. Rev. Appl. **14**, 024086 (2020).
[21]I. A. Golovchanskiy, N. N. Abramov, V. S. Stolyarov, M. Weides, V. V. Ryazanov, A. A. Golubov, A. V. Ustinov, and M. Y. Kupriyanov, Sci. Adv. **7**(25), eabe8638 (2021).
[22]S. Kezilebieke, M. N. Huda, V. Vaňo, M. Aapro, S. C. Ganguli, O. J. Silveira, S. Głodzik, A. S. Foster, T. Ojanen, and P. Liljeroth, Nature **588**, 424 (2020).
[23]S. Kezilebieke, O. J. Silveira, M. N. Huda, V. Vaňo, M. Aapro, S. C. Ganguli, J. Lahtinen, R. Mansell, S. van Dijken, A. S. Foster, and P. Liljeroth, Adv. Mater. **33**, 2006850 (2021).
[24]S. Jiang, J. Shan, and K. F. Mak, Nat. Mater. **17**, 406 (2018).
[25]Z. Wu, J. Yu, and S. Yuan, Phys. Chem. Chem. Phys. **21**, 7750 (2019).
[26]Y. Deng, Y. Yu, Y. Song, J. Zhang, N. Z. Wang, Z. Sun, Y. Yi, Y. Z. Wu, S. Wu, J. Zhu, J. Wang, X. H. Chen, and Y. Zhang, Nature **563**, 94 (2018).
[27]S. Jiang, L. Li, Z. Wang, K. F. Mak, and J. Shan, Nat. Nanotechnol. **13**, 549 (2018).
[28]Z. Zhang, J. Shang, C. Jiang, A. Rasmita, W. Gao, and T. Yu, Nano Lett. **19**, 3138 (2019).
[29]The quality factor of vortex can be obtained as $Q_v = P_{ideal}/P(f) = 1 + \omega_{vt}^2/\omega^2$[44] with $\omega_{vt} = \kappa/\eta$ and ω is the working frequency of the vortex.
[30]M. Golosovsky, M. Tsindlekht, and D. Davidov, Supercond. Sci. Technol. **9**(1), 1 (1996).
[31]B. D. Cuthbertson, M. E. Tobar, E. N. Ivanov, and D. G. Blair, Rev. Sci. Instrum. **67**, 2435 (1996).

[32]M. Harder, P. Hyde, L. Bai, C. Match, and C.-M. Hu, Phys. Rev. B **94**, 054403 (2016).
[33]A. D. O'Connell, M. Hofheinz, M. Ansmann, R. C. Bialczak, M. Lenander, E. Lucero, M. Neeley, D. Sank, H. Wang, M. Weides, J. Wenner, J. M. Martinis, and A. N. Cleland, Nature **464**, 697 (2010).
[34]F.-X. Sun, S.-S. Zheng, Y. Xiao, Q. Gong, Q. He, and K. Xia, Phys. Rev. Lett. **127**, 087203 (2021).
[35]N. Sakamoto, T. Akune, and Y. Matsumoto, Czech. J. Phys. Suppl. **46**, 1669 (1996).
[36]T. Akune, N. Sakamoto, Y. Matsumoto, and U. Ruppert, Physica C **426–431**, 666 (2005).
[37]M. M. Abu-Samreh, Physica B **321**, 368 (2002).
[38]T. Takayama and L. Rinderer, Physica B **107**, 431 (1981).
[39]Y. Liao and V. Galitski, Phys. Rev. B **100**, 060501 (2019).
[40]J. C. Swihart, J. Appl. Phys. **32**, 461 (1961).
[41]V. Petrovsky, T. Petrovsky, S. Kamlapurkar, and F. Dogan, J. Am. Ceram. Soc. **91**, 3590 (2008).
[42]J. J. Finley and B. S. Deaver, Solid State Commun. **36**, 493 (1980).
[43]R. E. Schwall, G. R. Stewart, and T. H. Geballe, J. Low Temp. Phys. **22**, 557 (1976).
[44]J. I. Gittleman and B. Rosenblum, Phys. Rev. Lett. **16**, 734 (1966).
[45]M. W. Coffey and J. R. Clem, Phys. Rev. Lett. **67**, 386 (1991).
[46]L. Bai, K. Blanchette, M. Harder, Y. P. Chen, X. Fan, J. Q. Xiao, and C. M. Hu, IEEE Trans. Magn. **52**, 1000107 (2016).
[47]N. Bloembergen and R. V. Pound, Phys. Rev. **95**, 8 (1954).
[48]B. I. Halperin and D. R. Nelson, J. Low Temp. Phys. **36**, 599 (1979).
[49]J. A. Galvis, E. Herrera, C. Berthod, S. Vieira, I. Guillamón, and H. Suderow, Commun. Phys. **1**, 30 (2018).
[50]H. Wang, X. Huang, J. Lin, J. Cui, Y. Chen, C. Zhu, F. Liu, Q. Zeng, J. Zhou, P. Yu, X. Wang, H. He, S. H. Tsang, W. Gao, K. Suenaga, F. Ma, C. Yang, L. Lu, T. Yu, E. H. T. Teo, G. Liu, and Z. Liu, Nat. Commun. **8**, 394 (2017).
[51]N. Kokubo, T. Asada, K. Kadowaki, and K. Takita, in *Proceedings of the 19th International Symposium on Superconductivity (ISS 2006)*, 2006, [Physica C **463–465**, 229 (2007)].
[52]X. Zhu, H. Ramezani, C. Shi, J. Zhu, and X. Zhang, Phys. Rev. X **4**, 031042 (2014).
[53]Z. Lin, H. Ramezani, T. Eichelkraut, T. Kottos, H. Cao, and D. N. Christodoulides, Phys. Rev. Lett. **106**, 213901 (2011).
[54]Y.-P. Wang, J. W. Rao, Y. Yang, P.-C. Xu, Y. S. Gui, B. M. Yao, J. Q. You, and C.-M. Hu, Phys. Rev. Lett. **123**, 127202 (2019).
[55]X.-Y. Lü, H. Jing, J.-Y. Ma, and Y. Wu, Phys. Rev. Lett. **114**, 253601 (2015).
[56]H. Xu, D. Mason, L. Jiang, and J. G. E. Harris, Nature **537**, 80 (2016).
[57]L. Feng, Z. J. Wong, R.-M. Ma, Y. Wang, and X. Zhang, Science **346**, 972 (2014).
[58]B. Peng, Ş. K. Özdemir, S. Rotter, H. Yilmaz, M. Liertzer, F. Monifi, C. M. Bender, F. Nori, and L. Yang, Science **346**, 328 (2014).
[59]Y. Cao and P. Yan, Phys. Rev. B **99**, 214415 (2019).
[60]R. P. Feynman, Found. Phys. **16**, 507 (1986).